行政院國家科學委員會補助專題研究計劃成果報告

※※※※※※※※※※※※※※※※※※※※※※※※※
※ ※
※ **PHASE TRANSITIONS IN A CU-14.5AL-9.0NI ALLOY** ※
※ ※
※※※※※※※※※※※※※※※※※※※※※※※※※

計劃類別： ☑個別型計劃 ❒整合型計劃

計劃編號：NSC90-2216-E-009-044

執行期間：90 年 08 月 01 日至 91 年 07 月 31 日

計劃主持人：劉增豐 教授

共同主持人：

本成果報告包括以下應繳之附件：

❒赴國外出差或研習心得報告一份

❒赴大陸地區出差或研習心得報告一份

❒出席國際學術會議心得報告及發表之論文各一份

❒國際合作研究計劃國外研究報告書一份

執行單位：國立交通大學材料科學及工程學系

中 華 民 國 91 年 12 月 16 日

行政院國家科學委員會補助專題研究計劃成果報告
PHASE TRANSITIONS IN A CU-14.5AL-9.0NI ALLOY

計劃編號：NSC90-2216-E-009-044

執行期限：90 年 08 月 01 日至 91 年 07 月 31 日

主持人：劉增豐　國立交通大學材料科學及工程學系

1. 中文摘要

在淬火狀態下，Cu-14.5Al-9.0Ni（wt.%）合金的顯微結構為（$D0_3$ + L-J）之混合相。當此合金在 500℃時效處理後，觀察到在層狀 γ′麻田散相中有高密度微細的B2析出物析出.其中γ′麻田散相是在淬火過程中經由 $D0_3$ → γ′麻田散相變化產生。隨著在 500℃的時效時間增加其一連續的相變化過程為 $D0_3$→($D0_3$+B2 析出物)→(α+$D0_3$+B2 析出物)→(α+γ_2+B2 析出物),這個實驗結果從未被其他學者在銅鋁鎳合金中發現過。

關鍵字：銅鋁鎳合金、相變化、γ′ 麻田散鐵、掃描及穿透式電子顯微鏡術、能量散佈分析儀

Abstract

In the as-quenched condition, the microstructure of the Cu-14.5Al-9.0Ni alloy was ($D0_3$+L-J) phases. During the early stage of isothermal aging at 500℃, a high density of the fine B2 precipitates was observed within the extremely thin lamellar γ_1' martensite, which was formed by a $D0_3 \rightarrow \gamma_1$' martensitic transformation during quenching. With increasing aging time at 500℃, the isothermal phase transition sequence was found to be $D0_3$→($D0_3$+B2 precipitate) →(α+$D0_3$+B2 precipitate)→(α+γ_2+B2 precipitate). This transition is quite different from that observed by other researchers.

Keywords: Cu-Al-Ni alloy, phase transformation, γ′ martensite, STEM, EDS

2.INTRODUCTION

The effects of nickel addition on the microstructural changes of Cu-Al binary alloys have been extensively studied [1-9]. According to those studies, when an alloy with a chemical composition of Cu- (14-15.1) wt. % Al- (3.1-7.7) wt. % Ni was solution heat-treated at a point in the single β phase (disordered body-centered cubic) region and then quenched into room-temperature water or iced-brine, the microstructure was single $D0_3$ phase [1-2], or $D0_3$ phase containing extremely fine 2H-type precipitates [3-4]. When the as-quenched alloy was aged at temperatures between 500 ℃ and 550 ℃ for a moderate duration and then quenched, γ_2 (Cu_9Al_4) particles firstly precipitated within the $D0_3$ matrix at the aging temperature, and the remaining $D0_3$ matrix was then transformed to γ_1' martensite during quenching [2,5]. With increasing aging time, the γ_2 particle grew and coalesced, and the remaining $D0_3$ matrix was completely transformed to a mixture of (α+β) phases at the aging temperature [5-6]. Consequently, the phase transition sequence at 500℃ and 550℃ was $D0_3$→($D0_3$+γ_2)→(α+β+γ_2). Besides, the γ_2 particle decomposed into B2 (NiAl) phase after aged at 500℃ for a long period [5].

To date, most examinations have focused on the Cu-Al-Ni alloys with Ni≦7.7 wt. % [1-8]. Little information concerning the microstructural development of the Cu-Al binary alloy with a higher nickel content has been provided. Therefore, the purpose of this study is an attempt to investigate the phase transition of the Cu- 14.5 wt. % Al- 9.0 wt. % Ni alloy by using optical microscopy (OM), scanning and transmission electron microscopy (STEM) and energy-dispersive X-ray spectrometry (EDS).

2. EXPERIMENTAL PROCEDURE

The alloy, Cu-14.5Al-9.0Ni (wt.%), was prepared in an air induction furnace by using 99.99% copper, 99.99% aluminum, and 99.95% nickel. The melt was chill cast into a 30x50x200-㎜ copper mold. After being homogenized at 1000℃ for 72 hours, the ingot was hot forged and rolled to a final thickness of 2.0 ㎜. The sheet was subsequently solution heat treated at 1050℃ for 1 hour and then rapidly quenched into iced water. The aging processes were performed at 500℃ for various times in a vacuum heat-treated furnace.

Electron microscopy specimens were prepared by means of a double-jet electropolisher with an electrolyte of 75 pct methanol and 25 pct nitric acid. The polishing temperature was kept in the range from -40℃ to -20℃,and the current density was kept in the range from $3.0x10^4$ to $4.0x10^4$ A/m^2. Electron microscopy was performed on a JEOL* 2000FX scanning transmission electron microscope (STEM) operating at 200 KV, using a double-tilting device. This microscope was equipped with a Link ISIS 300 energy-dispersive X-ray spectrometer (EDS) for chemical analysis. Quantitative analyses of elemental concentration for Cu, Al and Ni were made with the aid of a Cliff-Lorimer Ratio Thin Section method.

3. RESULTS

Figure 1(a) displays an optical micrograph of the present alloy after being solution heat-treated at 1050 ℃ for 1 hour followed by quenching. The micrograph reveals a single-phase microstructure. However, the TEM examinations indicated that in the as-quenched condition, the microstructure of the alloy was ($D0_3$ +L-J) phases. A typical microstructure is shown in Figures 1(b) through (e). This result is similar to that obtained by the present workers in the Cu-14.2Al-xNi (x = 4.3, 6.0 and 10.0 wt.%), Cu_2MnAl and $Cu_{2.2}Mn_{0.8}Al$ alloys [9-11].

Figure 2(a) is a bright-field (BF) electron micrograph of the alloy was aged at 500℃ for 20 minutes and then quenched. Figures 2(b) and (c), two selected-area diffraction patterns (SADPs) of the lamellar structure present in Figure 2(a), clearly indicate that these diffraction patterns consist of two sets of reflection reciprocal lattices. According the results of previous studies of Cu-Al-Ni alloys [5,7], one set derived from the B2 phase, and another derived from the γ_1' martensite with internal twins.

Figures 2(d) and (e), ($1\bar{2}1$) γ_1' and (100) B2 dark-field (DF) electron micrographs, clearly demonstrate the presence of the γ_1' martensite and the extremely fine B2 particles, respectively.

Figure 3(a) shows an optical micrograph of the alloy aged at 500℃ for 1 hour and then quenched, revealing that plate-like precipitates were formed within the matrix. Figure 3(b) is a BF electron micrograph of the aged alloy taken from a plate-like precipitate (marked as A) and its surrounding matrix (marked as B). Figure 3(c) is an SADP taken from the region A, shows that the microstructure of the plate-like precipitate was the mixture of (α+B2 precipitate). The orientation relationship between the B2 precipitate and the α phase was $(011)_{B2}//(111)_{\alpha}$ and $[11\bar{1}]_{B2}//[10\bar{1}]_{\alpha}$, which corresponds to the K-S orientation relationship [12]. In addition, the N-W orientation relationship between the B2 precipitate and the α phase could also be detected within another plate-like precipitate in the same specimen, as shown in Figure 3(d). Figure 3(e) is an SADP taken from the region B, indicating that the microstructure of the matrix was the mixture of (γ_1' martensite + B2 precipitate). The orientation relationship between the B2 precipitate and γ_1' martensite was $[001]_{B2}$ // $[10\bar{1}]_{\gamma 1'}$ and $(1\bar{1}0)_{B2}$ //$(121)_{\gamma 1'}$. Figure 3(f) is a (100) B2 DF electron micrograph, clearly showing that the B2 precipitates could be observed within both the γ_1' martensite and the disordered α phase, respectively.

With increasing the aging time at 500℃ for 24 hours, it is obviously revealed that many irregular and granular shaped particles formed within the matrix, as illustrated in Figure 4(a). Figures 4(b) and (c) show two SADPs taken from the region marked as "R" in Figure 4(a). Analyses of the diffraction patterns indicated that the microstructure was the mixture of (B2+γ_2) phases. The orientation relationship between the granular B2 particle and the γ_2 phase is cubic to cubic. This finding is similar to that observed by other researchers in the aged Cu-Al-Ni alloys [7]. Figure 4(d) is a (100) B2 DF electron micrograph, which clearly reveals the presence of the B2 particles. Figures 4(e) and (f) show that the orientation relationships between the B2 particle and the eutectoid α phase in regions "C" and "D", were determined to be K-S and N-W orientation relationships, respectively [12].

After prolonged aging time at 500℃, the stable microstructure of the alloy was a mixture of (α+γ_2+B2 precipitate) phases. Therefore, the phase transition sequence at 500℃ was found to be $D0_3$→ ($D0_3$+B2 precipitate) → (α+$D0_3$+B2 precipitate) → (α+γ_2+B2 precipitate). This transition significantly differs from that observed by other researchers [5].

4. DISCUSSION

Based on the above experimental results, some discussions are appropriate. During the early stage of isothermal aging at 500℃ in the present alloy, a high density of the extremely fine B2 particles were observed within the extremely thin lamellar γ_1' martensite, where the γ_1' martensite was formed by the $D0_3$ → γ_1' martensitic transformation during quenching. Prolonged aging time at 500℃ for a long period, the phase transition sequence was found to be $D0_3$→($D0_3$+B2 precipitate)→(α+$D0_3$+B2 precipitate)→(α+γ_2+B2 precipitate). This result is quite different from that observed by other workers in the Cu-14Al-4Ni alloy aged at 500℃ or 550℃ [5-6]. In order to clarify the characteristics of this transition in the present alloy aged at 500℃ isothermally, an TEM-EDS study was undertaken. The average atomic and weight percentages of the alloying elements examined by analyzing at least 10 different EDS spectra of each phase are listed in Table I. It is clearly seen in Table I that the aluminum and nickel contents in the B2 precipitate are much higher than those of the as-quenched alloy.

In our previous study, adding nickel to an Fe-23.2 at. % Al alloy could pronouncedly enhance the formation of the B2 and B2* phases, in which the latter is also a B2-type phase and enriched in both aluminum and nickel [13]. Therefore, it is reasonable to expect that a higher nickel addition in the Cu-14.5 wt. % Al alloy should favor the formation of the (Ni,Al)-riched B2 particles in the initial stage of aging at 500℃.Since the aluminum and nickel concentrations in the B2 precipitates are very high, along with the precipitation of the B2 precipitates, both of the aluminum and nickel content of the surrounding $D0_3$ matrix was depleted. In Table 3.1,it is also seen that the aluminum concentration in the remaining $D0_3$ matrix (i.e. γ_1' martensite) is about 12.31 wt. %, which is less than that of the as-quenched alloy in the present study. It is thus reasonable to believe that due to the lower aluminum content in the remaining $D0_3$ matrix, it would disadvantage the precipitation of the Al-rich γ_2 phase in the initial aging stage and cause the $D0_3$ matrix to transform to the γ_1' martensite during quenching in the present alloy.

Finally, it is worthwhile to mention that the alloy aged at 500℃ for a long period, the phase transition sequence was found to be $D0_3$→($D0_3$+B2 precipitate) → (α+$D0_3$+B2 precipitate)→(α+γ_2+B2 precipitate). However, in the previous studies [5-6], Singh et al. pointed out the phase transition sequence at 500℃ or 550℃ was $D0_3$→($D0_3$+γ_2)→(α+β+γ_2).This result is quite different from that observed by other workers in the Cu-Al-Ni alloy aged at 500℃ or 550℃.

5. CONCLUSIONS

On the basis of the above experimental results, the phase transition in the Cu- 14.5 wt. % Al- 9.0 wt. % Ni alloy could be summarized as follows:

(1) The higher nickel content in the Cu-Al-Ni alloy would enhance the precipitation of the B2 particles but disadvantage the formation of the γ_2 phase in the initial aging stage.

(2) With increasing the aging time at 500℃, the phase transition sequence was found to be $D0_3$ → ($D0_3$+B2) → ($D0_3$+B2+α) → (B2+α+γ_2.)

(3) Both K-S and N-W orientation relationships between the B2 particle and the disordered α matrix or the eutectoid α phase could be detected in the aged alloy.

6. ACKNOWLEDGEMENTS

The authors are pleased to acknowledge the financial support of this research by the National Science Council, Republic of China under Grant NSC90-2216-E-009-044.

7. REFERENCES

1.M.A. Dvorack, N. Kuwano, S. Polat, H. Chen and C.M. Wayman, *Scripta Metall.* 17 (1983) 1333-1336.

2.N. Zárubová, A. Gemperle and V. Novák, *Mater. Sci. Eng. A* A222 (1997) 166-174.
3.K. Otsuka, H. Sakamoto and K. Shimizu, *Trans. JIM* 20 (1979) 244-254.
4.K. Otsuka, H. Kubo and C.M. Wayman, *Metall. Trans* 12A (1981) 595-605.
5.J. Singh, H. Chen and C.M. Wayman, *Scripta Metall.* 19 (1985) 887-890.
6.J. Singh, H. Chen and C.M. Wayman, *Scripta Metall.* 19 (1985) 231-234.
7.Y.S. Sun, G.W. Lorimer and N. Ridley, *Metall. Trans. A* 21A (1990) 575-588.
8.V. Agafonov, P. Naudot, A. Dubertret and B. Dubois, *Scripta Metall.* 22 (1988) 489-494.
9.J. Tan and T.F. Liu, *Scripta Mater.* 43 (2000) 1083-1088.
10.S.C. Jeng and T.F. Liu, *Metall. Trans. A* 26A (1995) 1353-1365.
11.K.C. Chu and T.F. Liu, *Metall. Trans. A* 30A (1999) 1705-1716.
12.J. W. Edington, *Electron Diffraction in the Electron Microscope*, The MacMillan Press, London, vol. 2 (1975) pp. 116-117.
13. T.F. Liu, S.C. Jeng, and C.C. Wu, *Metall. Trans. A* 23A (1992) 1395-1401.

Table 1. Chemical compositions of the phases revealed by an Energy-Dispersive Spectrometer (EDS)

Heat treatment	Phase	Chemical Composition (wt.%)		
		Cu	Al	Ni
S.H.T.	($D0_3$+L-J)	76.90	14.25	9.01
500℃ 1 hr	B2 phase	36.45	23.97	39.63
	γ_1'-martensite	80.97	12.31	6.82
	disordered α phase	86.19	9.68	4.13
5000℃ 24hrs	B2 phase	24.99	29.52	45.76
	γ_2 phase	78.45	14.51	7.04
	disordered α phase	90.99	7.10	1.98

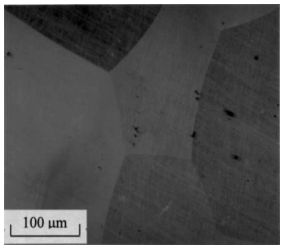

1(a)

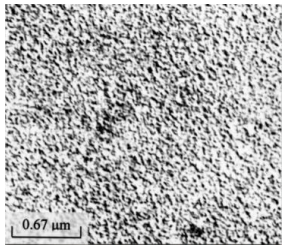

1(b)

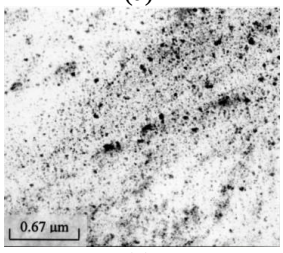

1(c)

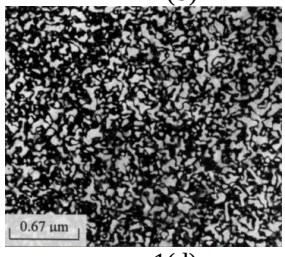

1(d)

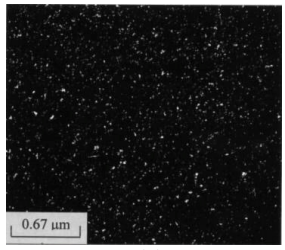

1(e)

Figure 1.Electron micrographs of the as-quenched alloy (a)OM, (b) BF, (c) (200) $D0_3$, (d) ($\bar{1}11$) $D0_3$, and (e) an L-J DF, respectively.

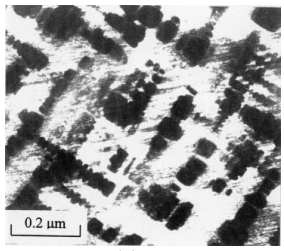

2(a)

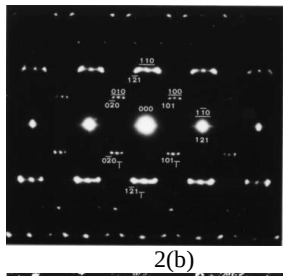
2(b)

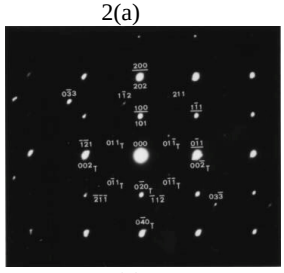
2(c)

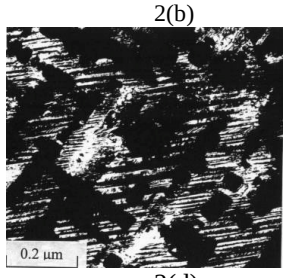

2(d)

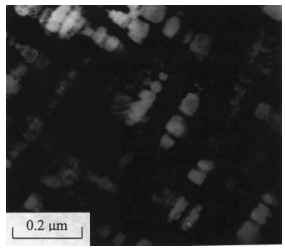

2(e)

Figure 2. Electron micrographs of the alloy aged at 500℃ for 20 minutes.(a) BF, (b) and (c) two SADPs. The zone axes of B2 phase, γ_1' martensite and internal twin are (b) [001], [$10\bar{1}$] and [$\bar{1}01$], and (c) [011], [$1\bar{1}\bar{1}$] and [$\bar{1}00$], respectively. (hkl = B2 phase, hkl = γ_1' martensite, hkl_T = internal twin). (d) and (e) ($1\bar{2}1$) γ_1' and (100)B2 DF.

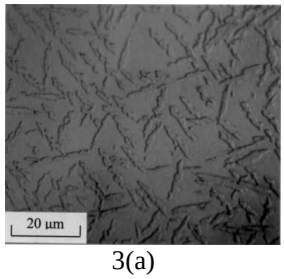

3(a)

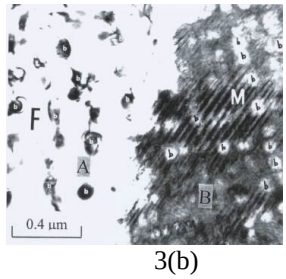

3(b)

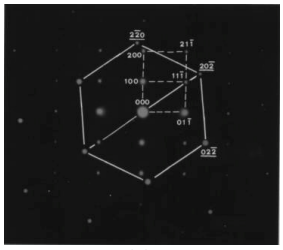

3(c)

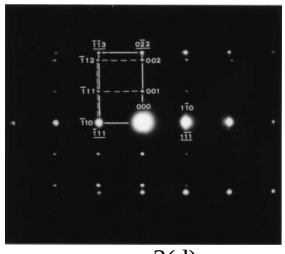

3(d)

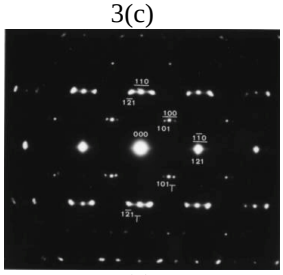

3(e)

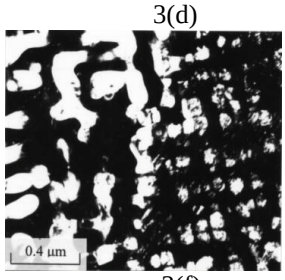

3(f)

Fig 3.Micrographs of the alloy aged at 500℃ for 1hour. (a) OM, (b)-(f) electron micrographs, (b) BF, (c) an SADP taken from the region A containing the granular B2 particle and its surrounding matrix in (b), (d) an SADP taken from the region B covering the irregularly shaped B2 particle and its contiguous matrix in (b) showing the K-S orientation relationship between B2 particle and disordered α phase: $(011)_{B2}//(111)_{\alpha}$ and $[11\bar{1}]_{B2}//[10\bar{1}]_{\alpha}$. (hkl = B2 phase, hkl = α phase). (d)showing the N-W orientation relationship between B2 particle and disordered α phase: $(100)_{B2}//(211)_{\alpha}$ and $[001]_{B2}//[0\bar{1}1]_{\alpha}$. (hkl = B2 phase, hkl = α phase). (e) an SADP showing the orientation relationship between the B2 precipitate and γ_1' martensite was $[001]_{B2}$ // $[10\bar{1}]_{\gamma1'}$ and $(1\bar{1}0)_{B2}$ //$(121)_{\gamma1'}$. (hkl = B2 phase, hkl = γ_1' martensite, hkl_T = internal twin). (f) (100) B2 DF.

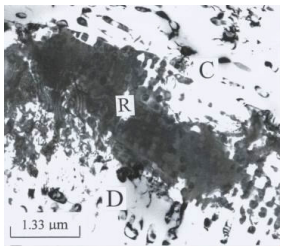

4(a)

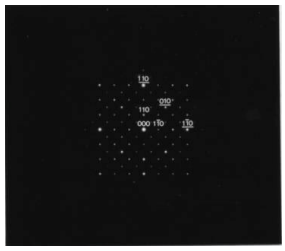

4(b)

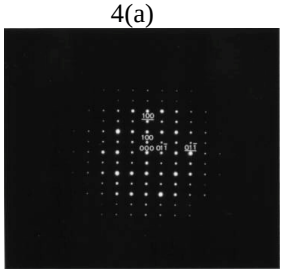

4(c)

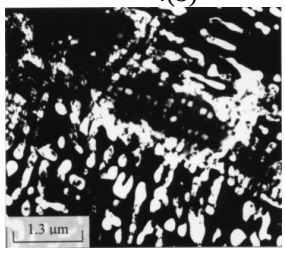

4(d)

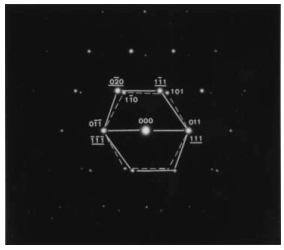

4(e)

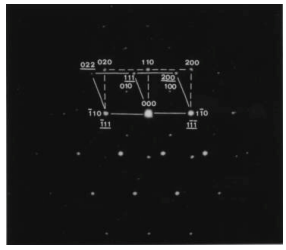

4(f)

Fig 4. Electron micrographs of the alloy aged at 500 ℃ for 24hours. (a) BF, (b) and (c) two SADPs. The zone axes of the B2 particle and the eutectoid γ_2 phase are (b)[001] and [001] and (c)[011] and [011], respectively. (hkl = B2 phase, hkl =γ_2 phase). (d)(100) B2 DF, (e)and(f)two SADPs showing the K-S and N-W orientation relationships between the B2 particle and eutectoid α phase: $(11\bar{1})_{B2}//(10\bar{1})_{\alpha}$ and $[011]_{B2}//[111]_{\alpha}$, $(001)_{B2}//(0\bar{1}1)_{\alpha}$ and $[1\bar{1}0]_{B2}//[1\bar{1}\bar{1}]_{\alpha}$, respectively. (hkl = B2 phase, hkl = α phase).